

# Changes in lumbosacral spinal nerve roots on diffusion tensor imaging in spinal stenosis

Zhong-jun Hou<sup>1,\*</sup>, Yong Huang<sup>1</sup>, Zi-wen Fan<sup>2</sup>, Xin-chun Li<sup>3</sup>, Bing-yi Cao<sup>1</sup>

1 Department of Radiology, the Second Affiliated Hospital of Guangzhou Medical University, Guangzhou, Guangdong Province, China  
2 Department of Orthopedics, the Second Affiliated Hospital of Guangzhou Medical University, Guangzhou, Guangdong Province, China  
3 Department of Radiology, the First Affiliated Hospital of Guangzhou Medical University, Guangzhou, Guangdong Province, China

\*Correspondence to:  
Zhong-jun Hou, 13694208683@163.com.

orcid:  
0000-0002-5916-7206 (Zhong-jun Hou)

doi: 10.4103/1673-5374.170317  
<http://www.nrronline.org/>

Accepted: 2015-09-10

## Abstract

Lumbosacral degenerative disc disease is a common cause of lower back and leg pain. Conventional T1-weighted imaging (T1WI) and T2-weighted imaging (T2WI) scans are commonly used to image spinal cord degeneration. However, these modalities are unable to image the entire lumbosacral spinal nerve roots. Thus, in the present study, we assessed the potential of diffusion tensor imaging (DTI) for quantitative assessment of compressed lumbosacral spinal nerve roots. Subjects were 20 young healthy volunteers and 31 patients with lumbosacral stenosis. T2WI showed that the residual dural sac area was less than two-thirds that of the corresponding normal area in patients from L<sub>3</sub> to S<sub>1</sub> stenosis. On T1WI and T2WI, 74 lumbosacral spinal nerve roots from 31 patients showed compression changes. DTI showed thinning and distortion in 36 lumbosacral spinal nerve roots (49%) and abruption in 17 lumbosacral spinal nerve roots (23%). Moreover, fractional anisotropy values were reduced in the lumbosacral spinal nerve roots of patients with lumbosacral stenosis. These findings suggest that DTI can objectively and quantitatively evaluate the severity of lumbosacral spinal nerve root compression.

**Key Words:** nerve regeneration; magnetic resonance imaging; diffusion tensor imaging; lumbosacral area; degeneration; nerve root; fractional anisotropy; neural regeneration

**Funding:** This study was supported by the Science and Technology Planning Project of Guangdong Province of China in 2012, No. 2012B031800232.

Hou ZJ, Huang Y, Fan ZW, Li XC, Cao BY (2015) Changes in lumbosacral spinal nerve roots on diffusion tensor imaging in spinal stenosis. *Neural Regen Res* 10(11):1860-1864.

## Introduction

Lumbosacral degenerative disc disease is the most common cause of pain in the lower back and legs. The most common levels of disc degeneration are at L<sub>4-5</sub> and L<sub>5</sub> to S<sub>1</sub> (Quint and Wilke, 2008; Hicks et al., 2009; Saleem et al., 2013). X-ray imaging plays a limited role in evaluating functional impairment associated with spinal cord degeneration (Quint and Wilke, 2008). Furthermore, the severity of lower back pain does not match the degree of disc degeneration and facet joint pathology on radiographs (Hicks et al., 2009).

Conventional magnetic resonance imaging (MRI), including T1-weighted imaging (T1WI) and T2-weighted imaging (T2WI), can image lumbosacral disc degeneration, but does not image the entire lumbosacral spinal nerve roots (LSNR). Three-dimensional (3D) MR radiculography is able to display the morphology of LSNR, although it has poor image rendering quality (Byun et al., 2012).

Diffusion weighted imaging (DWI) can provide valuable structural information and the apparent diffusion coefficient of the LSNR. DWI neuroimaging can visualize abnormalities such as nerve indentation, swelling, and transverse nerve direction through the foramen, and can quantitatively evaluate lumbar nerve entrapment in patients with foraminal stenosis. However, the resolution of the apparent diffusion coefficient map is unsatisfactory and the limited directions of the

gradient magnetic fields may affect the apparent diffusion coefficient value (Eguchi et al., 2010).

Diffusion tensor imaging (DTI) has been used to image nerve fiber tracts in the white matter of the central nervous system, and can also display peripheral nerve fibers (Li et al., 2013; Jang et al., 2014). Nevertheless, the application of DTI is less common for evaluation of LSNR morphology and pathology (Filippi et al., 2010; Eguchi et al., 2011). Clinical practice requires quantitative evaluation of the degree of trauma and recovery after treatment in LSNR (Arrigo et al., 2011). In the present study, we performed conventional MRI versus DTI in the lumbosacral spine to evaluate the LSNR in both healthy volunteers and patients with spinal stenosis. The aim of this study was to examine the potential of DTI for intuitive and quantitative assessment of the compressed LSNR.

## Materials and Methods

### Subjects

A total of 20 young healthy volunteers and 93 patients with lumbosacral stenosis were verified by physical examination in the Department of Orthopedics of the Second Affiliated Hospital of Guangzhou Medical University, China. For healthy volunteers, there were 14 males (mean age 23.3 ± 1.7 years; range: 21–27 years) and six females (22.8 ± 1.9 years; range: 21–26 years) as a control group.

### Conventional MRI

After signing informed consent, MRI scans were performed with a scanner (Signa 1.5T HDXT; General Electric, Milwaukee, WI, USA). For conventional examination, sagittal planes were oriented from the 10<sup>th</sup> thoracic vertebra to the coccyx on T1WI and T2WI, while axial T2WI scans were performed along the intervertebral spaces from L<sub>3</sub> to S<sub>1</sub> to assess intervertebral disc changes. Axial T2WI and DTI scans were then performed in horizontal orientation from the upper-middle part of the L<sub>2</sub> to the inferior margin of S<sub>1</sub> with 8-channel cardiac array coils.

The following scanning parameters were maintained for horizontal T2WI and DTI for orientation, slice thickness, number of slices, field of view, and zero gap. For axial T2WI, the scanning parameters were repetition time of 3,720.0–3,880.0 ms, echo time of 80.1–89.6 ms, slice thickness of 3 mm, field of view of 300 × 300 mm, matrix of 256 × 256, echo length of 16, number of slices of 50, signal excitations and acquisitions of 2, and scanning time from 2'44" to 3'22". For DTI, the scanning parameters were repetition time of 10,000–10,400 ms, echo time of 71.8–72.1 ms, matrix of 128 × 128, signal excitations and acquisitions of 8, diffusion factors at *b* values of 0 s/mm<sup>2</sup> and 400 s/mm<sup>2</sup>, 12 directions of diffusion gradients, and scanning time from 17'30" to 18'12" in echo planar imaging.

For post processing, images were processed using Functool 5.2.09 on the MRI host computer. First, on axial scans of intervertebral discs, the areas of the dural sacs were measured from L<sub>3</sub> to S<sub>1</sub> in both healthy volunteers and patients. At each level, the areas of the dural sacs were then measured three times and averaged.

### Patient selection

Patients who exhibited the following symptoms were selected: intermittent claudication, numbness, and weakness that could be relieved by bed rest and bending motion or aggravated by extension of the legs. In a clinical test, patients exhibited altered sensation disturbances in the back and legs, weakening or disappearance in ankle reflection, and atrophy in the buttocks and legs. One patient exhibited cauda equina syndrome characterized by serious low back pain, radicular pain in both legs, numbness around the anus, urine retention, and fecal incontinence. With respect to accessing standards, only those patients without a metal frame of the vertebral body and dural sac area less than two-thirds of that at the corresponding normal intervertebral spaces were included in this study (Feng et al., 2000). Thirty-one patients out of 93 exhibited this requirement. The lesion group contained 18 males (mean 51.0 ± 9.1 years; range: 33–63 years) and 13 females (62.5 ± 13.9 years; range: 39–80).

### DTI data analysis

In post processing of DTI data, after comparing the shape and contours of the dural sac on axial T2WI and DTI and ruling out image deformation, we selected one of 12 groups of DTI with 50 images, and then reconstructed the spinal nerves and ganglia on the maximum intensity projection.

DWI neuroimaging in one direction was used as the reference for DTI tractography. To mark the nerve roots at the cauda equina and the dorsal root ganglia, the fractional anisotropy (FA) values of LSNR were measured in triplicate at each site; the positions were recorded for selecting the region of interest and tracking LSNR. The 'seed' and 'target' mode were used by referring the regions of interest of the proximal and distal ends of the LSNR on 3D axial DTI images. Images of the LSNR from L<sub>3</sub> to S<sub>1</sub> on both sides were reconstructed using an FA threshold of 0.18.

### Statistical analysis

Data were analyzed using SPSS 11.5 software (SPSS, Chicago, IL, USA). The dural sac area, between two-thirds of the normal and the narrowed lumbosacral canal, and FA values between healthy volunteers and patients in the lesion group were compared using the Student's *t*-test. A *P* value less than 0.05 was considered statistically significant.

## Results

### Dural sac area in healthy volunteers and patients with lumbosacral stenosis

In 20 healthy volunteers, the dural sac areas of the axial lumbosacral canals were 188.7 ± 45.0 mm<sup>2</sup>, 174.6 ± 44.0 mm<sup>2</sup>, and 156.6 ± 44.5 mm<sup>2</sup> at L<sub>3-4</sub>, L<sub>4-5</sub>, and L<sub>5</sub> to S<sub>1</sub>, respectively, and 173.0 ± 46.1 mm<sup>2</sup> on average. The residual dural sac area of the lumbosacral canal was reduced in patients with lumbosacral stenosis (98.9 ± 25.6 mm<sup>2</sup>) to two-thirds of the dural sac area of normal persons (115.3 ± 30.7 mm<sup>2</sup>) (*t* = 4.719, *P* = 0.000).

### FA values of LSNR from L<sub>2</sub> to S<sub>1</sub> between healthy volunteers and patients with lumbosacral canal stenosis

The mean FA value was higher in healthy volunteers (0.332 ± 0.074) than that in patients with lumbosacral canal stenosis (0.304 ± 0.085) (*P* = 0.000).

### Neuroimaging and tractography of LSNR

In healthy volunteers, DWI showed symmetrical or almost symmetrical LSNR from L<sub>3</sub> to S<sub>1</sub>, which was very clear from the bifurcation of the LSNR in the cauda equina to the dorsal ganglia. The LSNR from L<sub>2</sub> to S<sub>1</sub> was observed completely on DTI tractography, which corresponded to DWI neuroimaging and normal anatomy (**Figure 1**) (Arslan et al., 2011). Lumbosacral degeneration was seen in 74 LSNR of patients with spinal stenosis on T1WI and T2WI. On DTI tractography, 36 LSNR (49%) were thin and distorted, while 17 LSNR (23%) were ruptured (**Figures 2 and 3**). Morphologically, the most evident signs were asymmetry and distortion of the LSNR. Overall, these data suggest that the compression state of the ruptured LSNR on DTI was more serious than that of thinning and distortion observed with T1WI and T2WI.

## Discussion

### Spinal degeneration and spinal stenosis

Senocak et al. (2009) reported that the cauda equina conduction time was significantly prolonged in lumbar spinal stenosis.

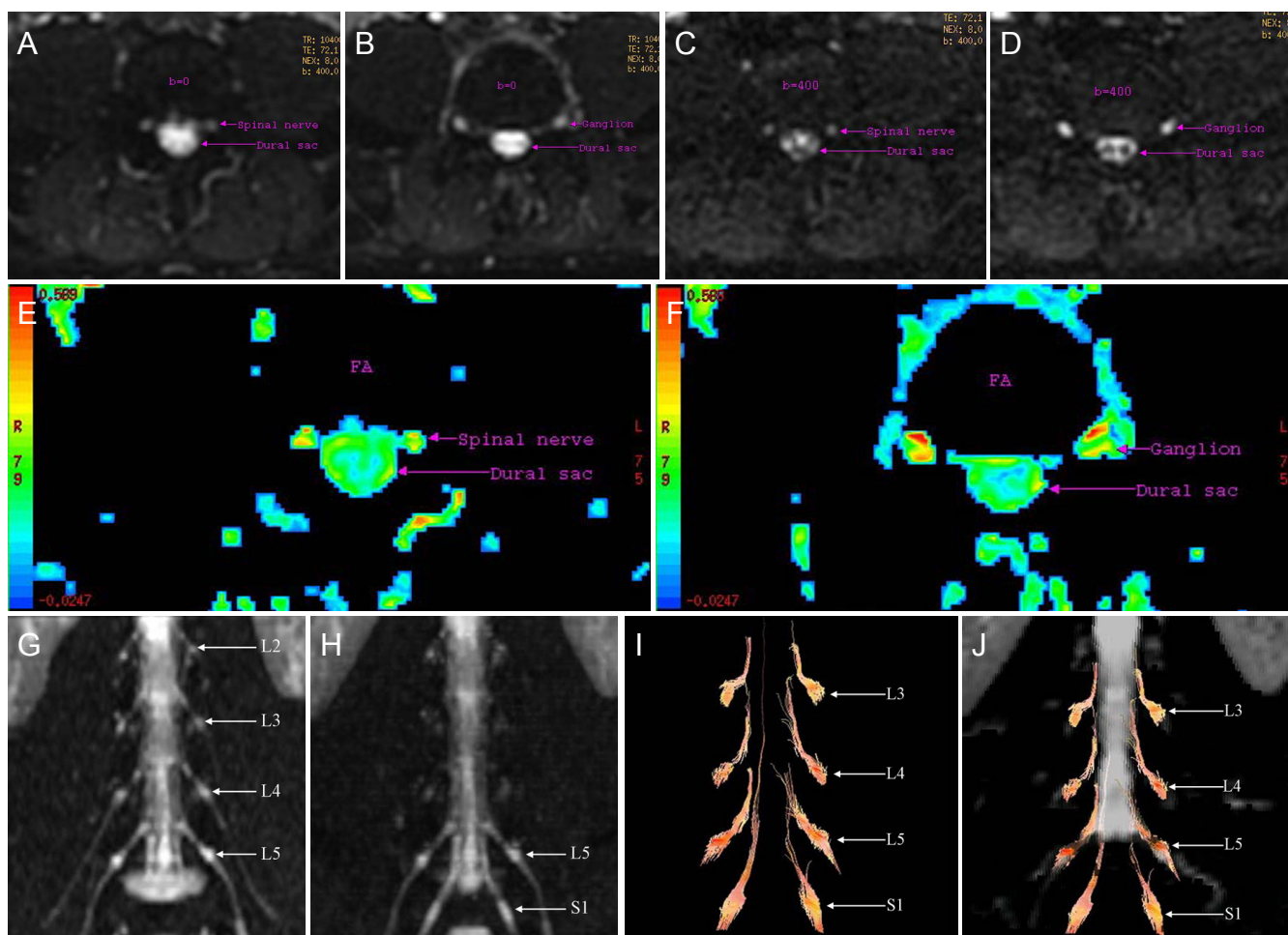


**Figure 1** Images of LSNR of a 22-year-old male healthy volunteer.

(A–J) Axial scans of echo planar imaging showing the proximal LSNR, ganglion of the spinal nerve, and the dural sac at L<sub>5</sub> to S<sub>1</sub> on A and B ( $b = 0 \text{ s/mm}^2$ ) and on C and D ( $b = 400 \text{ s/mm}^2$ ). The corresponding FA images are shown on E and F. DWI showing the LSNR and the corresponding ganglia on maximum intensity projection reconstruction of a thin slice from L<sub>2</sub> to L<sub>5</sub> on G and from L<sub>5</sub> to S<sub>1</sub> on H. Diffusion tensor imaging showing the LSNR and the corresponding ganglia from L<sub>3</sub> to S<sub>1</sub> without coregistration with the reconstruction of DWI with a  $b$  value selected at  $0 \text{ s/mm}^2$  on I, and with coregistration with the reconstruction of DWI with a  $b$  value selected at  $0 \text{ s/mm}^2$  on J. LSNR: Lumbosacral spinal nerve roots; FA: fractional anisotropy; DWI: diffusion weighted imaging.

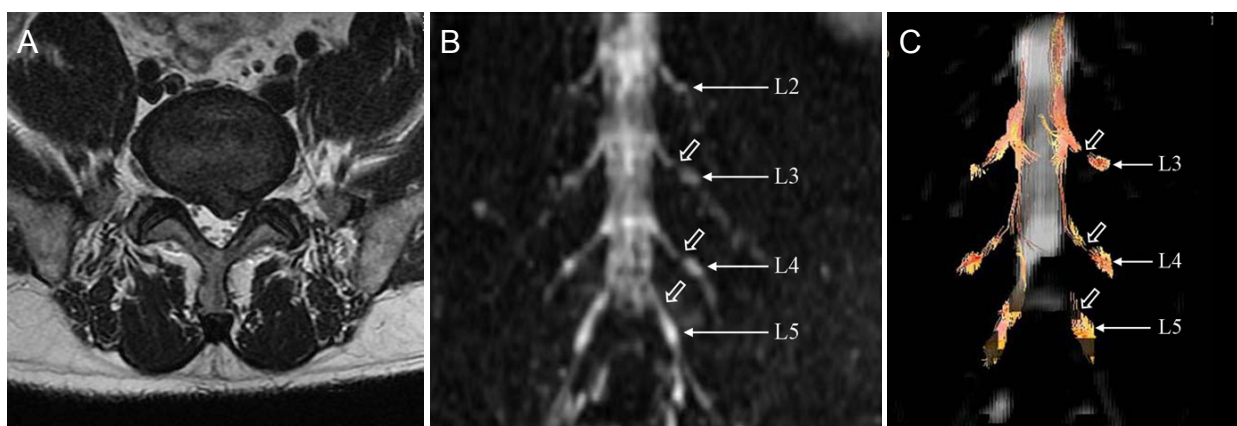


**Figure 2** Changes in the LSNR of a 56-year-old male patient with spinal stenosis.

(A–C) Axial image of T2-weighted imaging showing bulging and left posterolateral protrusion of the intervertebral disc at L<sub>2</sub> to S<sub>1</sub> on A. Diffusion weighted imaging showing thinning of the left proximal L<sub>5</sub> LSNR (empty arrow) and abruption of the left LSNR at L<sub>3</sub> and L<sub>4</sub> due to compression of the corresponding bulging disc (empty arrow). Diffusion tensor imaging showing distortion and abruption of the left proximal L<sub>5</sub> LSNR and abruption of the left LSNR at the L<sub>3</sub> and L<sub>4</sub> levels (empty arrow). LSNR: Lumbosacral spinal nerve roots.

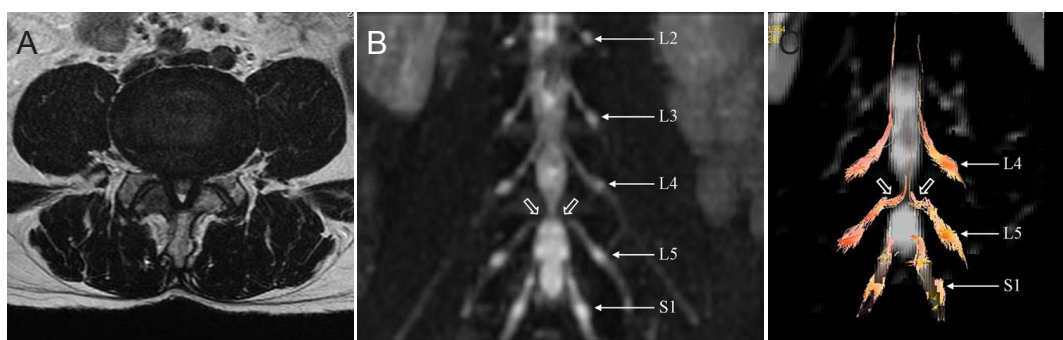


**Figure 3** Changes in the LSNR of a 59-year-old male patient with spinal stenosis.

(A–C) Axial images of T2-weighted imaging showing extrusion of the intervertebral disc at L<sub>4-5</sub>. Diffusion weighted imaging showing distortion of the proximal parts of the bilateral L<sub>5</sub> LSNR (empty arrow) and dural sac stenosis. Diffusion tensor imaging showing downward displacement and distortion of the bilateral proximal L<sub>5</sub> LSNR (empty arrow). LSNR: Lumbosacral spinal nerve roots.

When the central canal area was less than 1.5 cm<sup>2</sup>, a delay of cauda equina conduction may occur. Demyelination was previously reported in the compressed cauda equina (Senocak et al., 2009). Feng et al. (2000) also reported that the cauda equina showed high signal on MRI, with normal axons by light microscope, but worm-eaten changes in the myelin sheath without evidence of changes in polyribosomes and rough endoplasmic reticulum by electron microscope in dogs with 25% canal stenosis at 12 weeks of recovery. In dogs with 50% canal stenosis, there was evidence of high signal on MRI, with varied axonal diameters, partial separation, and vacuolation by light microscope, and myelin degeneration, axonal atrophy, and metachromatic granules in Schwann cell membrane by electron microscope at 12 weeks of recovery. In dogs with 75% canal stenosis, there was evidence of high signal on MRI and disappearance of normal structures by light microscopy, and lamellar myelin disorders and axon loss by electron at 12 weeks of recovery. Taken together, compression leads to deterioration in the function and histology of the cauda equina.

#### Sensitivity of FA in detecting spinal degeneration

FA is an important indicator for describing the degree of anisotropy on DTI (Filler, 2009; Jambawalikar et al., 2010). An FA of zero represents isotropic diffusion, while an FA of 1 represents only linear diffusion. FA values in nerve fibers of the human body range from 0.2–0.8 (Jambawalikar et al., 2010). In the present study, the mean normal FA value of the LSNR was  $0.332 \pm 0.074$ . Anatomically, from the L<sub>1</sub> to L<sub>5</sub> level, the average angle was 40° (range 37–41°) between the LSNR and the dural sac. At the S<sub>2</sub> level, the angle sharply reduces to  $22 \pm 4^\circ$  on average, and tends to be smaller in the following spinal nerves in the sacral canal (Cohen et al., 1990).

Previous studies have used DTI for anatomical assessment of spinal nerves. For example, spinal nerve imaging by DWI could visualize anatomical structures from the separation of the LSNR to the dorsal ganglia. FA values of the spinal nerves were also significantly lower after sciatic neuropathy compared with controls. Furthermore, FA values in the sciatic nerve were correlated with disability scores and electrophysiological parameters of axonal damage at baseline and at 6 months after the initial DTI scan (Mathys et al., 2013). The changes in FA values were strongly correlated with his-

tological changes, including axon and myelin regeneration (Takagi et al., 2009; Morisaki et al., 2011), and indicated that axon membranes played a major role in anisotropic water diffusion and that myelination could modulate the degree of anisotropy (Takagi et al., 2009). In the present study, the FA value of the LSNR was lower in areas of lumbar stenosis, in which the LSNR is compressed over a long period with demyelination and axonal degeneration (Feng et al., 2000). These findings are consistent with previous studies (Takagi et al., 2009; Morisaki et al., 2011; Mathys et al., 2013).

#### Significance of tractography in assessing the changes in LSNR

Lumbosacral spine MRI clearly shows the structures of the spinal canal and characteristics of the spinal nerves on T1WI and T2WI. DWI can clearly visualize the shape of the spinal nerves and the nerve ganglia in maximum intensity projection mode (Zhang et al., 2009). In the present study, we used a group of DTI images in one direction for DWI to reduce the misregistration between DTI and DWI.

The axial scanning of the two-dimensional T2WI in our study matched that of DTI with respect to range, thickness, and orientation for comparison of the spinal structures. The separation points of the LSNR and the dorsal ganglia were visible on DWI. This allowed us to mark the slice position of the LSNR and apply it to the axial images of DTI for selecting the ‘seed’ and ‘target’ to reconstruct the LSNR. Our results confirmed that the LSNR could be displayed clearly and symmetrically in normal volunteers from L<sub>3</sub> to S<sub>1</sub> on DTI. However, in patients with lumbosacral stenosis, LSNR had a varied appearance including thinning, distortion, and abruptness. Asymmetry and distortion were the main morphological changes in LSNR.

#### Study limitations

This study compared LSNR between normal volunteers and lumbar stenosis patients using DTI. DTI has high potential for displaying the morphology and histology of the LSNR. However, image distortion can occur with DTI as a result of eddy currents, cerebrospinal fluid motion, and physiological movement (Wang et al., 2011; Middleton et al., 2014). Simultaneously, the impact of the intervertebral discs should

be considered during reconstruction of the LSNR (Yang et al., 2007), while the presence of the cauda equina will affect observation of the LSNR (Hou et al., 2013). Indeed, the finding of abruptness of the LSNR on tractography does not indicate disconnection of the spinal nerves, but rather loss on tractography tracing due to the lower FA (Eguchi et al., 2010). An indicator of the dural sac area may not fully reflect the real severity of LSNR compression, as the degree of stenosis of the lateral recess plays a more important direct role, while the lateral recess on one side or both sides is difficult to evaluate quantitatively and repeatedly. Nevertheless, the dural sac area represents an aspect of the severity of compression in the cauda equina.

In clinical practice, after surgery the quality of DTI in reexamination is often diminished by the metal instrument fixed on the vertebral pedicles. In addition, scanning with DTI is time-consuming when the scanning direction is perpendicular to the spinal canal. Furthermore, the tractography findings did not totally match the changes in LSNR on T1WI and T2WI, with nearly 30% false negative results. The quality of tractography and spatial resolution of the images were based mainly on the skill and experience of the operator. Thus, to assure the quality of DTI, future studies are required to reduce the scan time and improve the reconstruction mode of tractography for assessment of LSNR.

**Acknowledgments:** We thank technician Shu-xin Li for his instruction and help in MRI scans in both volunteers and patients in the Department of Radiology of the Second Affiliated Hospital of Guangzhou Medical University in China.

**Author contributions:** ZJH, YH, ZWF and XCL participated in study design. ZJH, XCL and BYC did literature search. ZJH, YH and BYC performed experiments. ZJH, YH and ZWF collected data. ZJH and ZWF analyzed the data. ZJH wrote the paper. ZJH and XCL reviewed the paper. All authors approved the final version of the paper.

**Conflicts of interest:** None declared.

**Plagiarism check:** This paper was screened twice using Cross-Check to verify originality before publication.

**Peer review:** This paper was double-blinded, stringently reviewed by international expert reviewers.

## References

- Arrigo RT, Kalanithi P, Boakye M (2011) Is cauda equina syndrome being treated within the recommended time frame? *Neurosurgery* 68:1520-1526.
- Arslan M, Cömert A, Açar H, Özdemir M, Elhan A, Tekdemir İ, Tubbs S, Attar A, Uğur H (2011) Lumbosacral intrathecal nerve roots: an anatomical study. *Acta Neurochir (Wien)* 153:1435-1442.
- Byun WM, Ahn SH, Ahn MW (2012) Value of 3D MR lumbosacral radiculography in the diagnosis of symptomatic chemical radiculitis. *Am J Neuroradiol* 33:529-534.
- Cohen MS, Wall EJ, Brown RA, Rydevik B, Garfin SR (1990) 1990 AcroMed Award in basic science. Cauda equina anatomy. II: Extrathecal nerve roots and dorsal root ganglia. *Spine (Phila Pa 1976)* 15:1248-1251.
- Eguchi Y, Ohtori S, Orita S, Kamoda H, Arai G, Ishikawa T, Miyagi M, Inoue G, Suzuki M, Masuda Y, Andou H, Takaso M, Aoki Y, Toyone T, Watanabe A, Takahashi K (2011) Quantitative evaluation and visualization of lumbar foraminal nerve root entrapment by using diffusion tensor imaging: preliminary results. *Am J Neuroradiol* 32:1824-1829.
- Eguchi Y, Ohtori S, Yamashita M, Yamauchi K, Suzuki M, Orita S, Kamoda H, Arai G, Ishikawa T, Miyagi M, Ochiai N, Kishida S, Masuda Y, Ochi S, Kikawa T, Takaso M, Aoki Y, Toyone T, Suzuki T, Takahashi K (2010) Clinical applications of diffusion magnetic resonance imaging of the lumbar foraminal nerve root entrapment. *Eur Spine J* 19:1874-1882.
- Feng JG, Han YT, Wang F (2000) Comparative observation of MRI and histology of delayed graded compression of the dog cauda equina. *Zhonghua Fangshe Xue Zazhi* 34:208-211.
- Filippi C, Andrews T, Gonyea J, Linnell G, Cauley K (2010) Magnetic resonance diffusion tensor imaging and tractography of the lower spinal cord: application to diastematomyelia and tethered cord. *Eur Radiol* 20:2194-2199.
- Filler A (2009) Magnetic resonance neurography and diffusion tensor imaging: origins, history, and clinical impact of the first 50,000 cases with an assessment of efficacy and utility in a prospective 5000-patient study group. *Neurosurgery* 65:A29-43.
- Hicks GE, Morone N, Weiner DK (2009) Degenerative lumbar disc and facet disease in older adults: prevalence and clinical correlates. *Spine* 34:1301-1306.
- Hou ZJ, Huang Y, Fan ZW, Cao BY (2013) The research of diffusion tensor imaging of magnetic resonance imaging in normal cauda equina. *Yixue Yingxiang Xue Zazhi* 23:371-375.
- Jambawalikar S, Baum J, Button T, Li H, Geronimo V, Gould E (2010) Diffusion tensor imaging of peripheral nerves. *Skeletal Radiol* 39:1073-1079.
- Jang SH, Chang PH, Kim YK, Seo JP (2014) Anatomical location of the frontopontine fibers in the internal capsule in the human brain: a diffusion tensor tractography study. *Neuroreport* 25:117-121.
- Li X, Chen J, Hong G, Sun C, Wu X, Peng MJ, Zeng G (2013) In vivo DTI longitudinal measurements of acute sciatic nerve traction injury and the association with pathological and functional changes. *Eur J Radiol* 82:e707-e714.
- Mathys C, Aissa J, Zu Hörste GM, Reichelt DC, Antoch G, Turowski B, Hartung HP, Sheikh KA, Lehmann HC (2013) Peripheral neuropathy: assessment of proximal nerve integrity by diffusion tensor imaging. *Muscle Nerve* 48:889-896.
- Middleton DM, Mohamed FB, Barakat N, Hunter LN, Shellikeri S, Finsterbusch J, Faro SH, Shah P, Samdani AF, Mulcahey MJ (2014) An investigation of motion correction algorithms for pediatric spinal cord DTI in healthy subjects and patients with spinal cord injury. *Magn Reson Imaging* 32:433-439.
- Morisaki S, Kawai Y, Umeda M, Nishi M, Oda R, Fujiwara H, Yamada K, Higuchi T, Tanaka C, Kawata M, Kubo T (2011) In vivo assessment of peripheral nerve regeneration by diffusion tensor imaging. *J Magn Reson Imaging* 33:535-542.
- Quint U, Wilke HJ (2008) Grading of degenerative disk disease and functional impairment: imaging versus patho-anatomical findings. *Eur Spine J* 17:1705-1713.
- Saleem S, Aslam HM, Rehmani MAK, Raees A, Alvi AA, Ashraf J (2013) Lumbar disc degenerative disease: disc degeneration symptoms and magnetic resonance image findings. *Asian Spine J* 7:322-334.
- Senocak Ö, Hürel DM, Sener U, Ugurel B, Öztura I, Ertekin C (2009) Motor conduction time along the cauda equina in patients with lumbar spinal stenosis. *Spine* 34:1410-1414.
- Takagi T, Nakamura M, Yamada M, Hikishima K, Momoshima S, Fujiyoshi K, Shibata S, Okano HJ, Toyama Y, Okano H (2009) Visualization of peripheral nerve degeneration and regeneration: monitoring with diffusion tensor tractography. *Neuroimage* 44:884-892.
- Wang ZJ, Seo Y, Chia JM, Rollins NK (2011) A quality assurance protocol for diffusion tensor imaging using the head phantom from American College of Radiology. *Med Phys* 38:4415-4421.
- Yang HT, Wang RF, Wang J, Gao XL, Li FT, Zhang HD, Xia LM, Wang CY (2007) Clinical application of MR diffusion tensor imaging in lumbar disc annulus fibrosis. *Zhonghua Fangshe Xue Zazhi* 41:1100-1103.
- Zhang Z, Song L, Meng Q, Li Z, Pan B, Yang Z, Pei Z (2009) Morphological analysis in patients with sciatica: a magnetic resonance imaging study using three-dimensional high-resolution diffusion-weighted magnetic resonance neurography techniques. *Spine (Phila Pa 1976)* 34:E245-250.

Copyedited by Dean J, Raye W, Yu J, Qiu Y, Li CH, Song LP, Zhao M